

FACTS IMPACTS ON INDUCTION GENERATOR DRIVEN BY WIND TURBINE

Youssef A. Mobarak

Electrical Engineering Department, Faculty of Energy Engineering, South Valley University, Aswan, Egypt

(Received February 7, 2012 Accepted March 8, 2012)

This paper presents the effect of the combination between SVC and STATCOM on the performance of an induction generator driven by wind turbine. Also the comparison is made between the performances of the wind farm equipped by SVC, STATCOM and the combination in between them to improve the wind farm power system performance. The simulation results show that both of the devices enhance the power system performance during and after disturbance, especially when the network is weak. The results show the effect of the combination between SVC & STATCOM connected on bus #3. The combination between SVC & STATCOM enhances the power system performance.

KEYWORDS: *Induction Generator, FACTS, Wind Turbine.*

1. INTRODUCTION

In recent years generation of electricity using wind power has received considerable attention worldwide. Induction machines are mostly used as generators in wind power based generations. Since induction machines have a performance problem as they draw very large reactive currents during fault condition, reactive power compensation can be provided to improve performance. This part presents general review and previous work of wind turbine and wind generators [1-5]. Also, it is intended to provide an overview of some well known FACTS controllers in order to provide the merits and applications of FACTS to the operations of transmission and distribution systems. The proposed shunt FACTS devices are Static VAR Compensator SVC and Static Synchronous Compensator STATCOM [5-9]. There exists a large collection of literature on the modeling of wind energy conversion systems more specifically on the modeling of individual system components of a wind energy conversion system. A wind energy conversion system is mainly comprised of two subsystems, namely a wind turbine part and an electric generator part. Detailed descriptions of these concepts can be found in text books on wind energy [1, 2]. A summary of the typical wind turbine models and their control strategies is presented in [1]. Most of the models used to represent a wind turbine are based on a non linear relationship between rotor power coefficient and linear tip speed of the rotor blade [1-5].

A very large wind farm contains hundreds of wind turbines connected together by an intricate collector system. Though each WT of a wind farm may not critically impact the power system, a wind farm has significant impact on the associated power system during severe disturbances [10]. It is not practical to represent all wind turbines to perform a simulation study; a simplified equivalent model is required. It also helps that there is no mutual interaction between wind turbines with well-tuned converters in

a wind farm [11, 12]. The most popular type of wind turbines installed today are variable speed wind turbines that feature improved power quality and speed control and reduced mechanical stresses. Under the same circumstances, the power generated by variable speed wind turbines is greater than that generated by the fixed speed wind turbines [8]. Majority of the wind power based DG technologies employ induction generators instead of synchronous generators, for the technical advantages of induction machines like: reduced size, increased robustness, lower cost, and increased electromechanical damping. Wind turbine induction generator WTIG can be viewed as a consumer of reactive power. Its reactive power consumption depends on active power production. Further, induction generators draw very large reactive currents during fault occurrence [13].

Flexible AC Transmission Systems FACTS such as SVC and STATCOM are being used extensively in power systems because of their ability to provide flexible power flow control [14]. The main motivation for choosing SVC or STATCOM in wind farms is its ability to provide bus bar system voltage support either by supplying and/or absorbing reactive power into the system. The applicability of FACTS in wind farms has been investigated and the results from early studies indicate that it is able to supply reactive power requirements of the wind farm under various operating conditions, thereby improving the steady-state stability limit of the network. Transient and short-term generator stability conditions can also be improved when a STATCOM has been introduced into the system as an active voltage/var supporter [14-16]. The SVC can be considered as a shunt impedance determined by the parallel connection of the capacitor and the effective inductance of the thyristor controlled reactor [17]. The reactive power injection capability of the SVC is mainly applied to control voltage and damp oscillations, but also to improve the steady state power flow and transient stability [18]. In [19] it is suggested to use FACTS devices such as SVC and STATCOM to improve the stability in wind farm.

Generally, stability means the capability of power system to hold synchronism during occurrence of a severe transient disturbance such as fault in equipment and transmission line or loss of generation or lumped load. Application of STATCOM for stability improvement has been discussed in the literature [20-24]. A comparative study between the conventional SVC and STATCOM in damping power system oscillation is given in [20]. The results show the superiority of STATCOM-based controller over SVC-based controller in increasing the damping of low frequency oscillations. A robust controller for providing damping to power system through STATCOM is presented in [25]. The loop-shaping technique has been employed to design the controllers. It was observed that a robust controller in the speed loop, with nominal voltage feedback, effectively damps the electromechanical oscillations for a wide range of operating conditions. Two new variable structure fuzzy control algorithms for controlling the reactive component of the STATCOM current are presented in [23]. The signal input to the proposed controller is obtained from a combination of generator speed deviation and STATCOM bus voltage deviation. Nonlinear control theory has been applied to design STATCOM damping controller in [24].

This paper introduces the impact of a combination of SVC & STATCOM in improving the performance of WTIG on the occurrence of disturbances such as the change of wind speed, phase-to-phase ground fault, three-phase to ground fault, sudden injection or rejection of an inductive load and the connection of a plant consisting of an

induction motor and a resistive load. The study is based on the three phase non-linear dynamic simulation, utilizing the SimPowerSystems Blockset for use with MATLAB/SIMULINK. Simulation results are presented to show the improved performance of a distributed network embedded with WTIGs under severe disturbances.

2. STUDIED SYSTEM AND MODELING

The mathematical models of wind turbine and wind generators (three phase squirrel cage induction generator) are presented in this paper. The proposed shunt FACTS devices are SVC and STATCOM. The general concepts of FACTS controllers modeling are explained in steady-state and transient stability. The wind farm using Induction Generators IG driven by variable-pitch wind turbines test system is utilized. The effect of some system parameters like rating of capacitor bank, SVC rating, STATCOM rating and transmission line length, on performance of induction generator driven by wind turbine is studied and presented.

2.1 Wind Turbine Model

The wind turbine model employed in the present study is based on the steady-state power characteristics of the turbine. The stiffness of the drive train is infinite and the friction factor and the inertia of the turbine are combined with those of the generator coupled to the turbine. The wind turbine mechanical power output is a function of rotor speed as well as the wind speed and is expressed as:

$$P_m = C_p(\lambda, \beta) \frac{\rho A}{2} V_{wind}^3 \quad (1)$$

Normalizing (1) in the per unit (pu) system as:

$$P_{m-pu} = k_p C_{p-pu} V_{Wind-pu}^3 \quad (2)$$

A generic equation is used to model $C_p(\lambda, \beta)$. This equation, based on the modeling turbine characteristics is:

$$C_p(\lambda, \beta) = C_1 \left(\frac{C_2}{\lambda_i} - C_3 \beta - C_4 \right) e^{\frac{-C_5}{\lambda_i}} + C_6 \lambda \quad (3)$$

With

$$\frac{1}{\lambda_i} = \frac{1}{\lambda + 0.08\beta} - \frac{0.035}{\beta^3 + 1} \quad (4)$$

The coefficients C_1 to C_6 are constants: $C_1=0.5176$, $C_2= 116$, $C_3=0.4$, $C_4=5$, $C_5=21$, and $C_6=0.0068$. In this research a constant pitch angle β is used and its value is assigned as zero, the based speed is selected at 9m/sec. The turbine power characteristics of the model employed in this paper presented in Fig. (1) shows how PWT varies with rotor speed for different wind speeds. The optimum tip speed ratio curve gives the highest efficiency points for PWT. As seen from figure, rated power 3MW (1p.u) occurs at rated wind speed of 9m/s. In dynamic simulations, the electricity-producing wind turbine is treated as a complex electromechanical system consisting of the induction generator, the drive train system and the rotating wind turbine. Its modular diagram is given in Fig. (2)

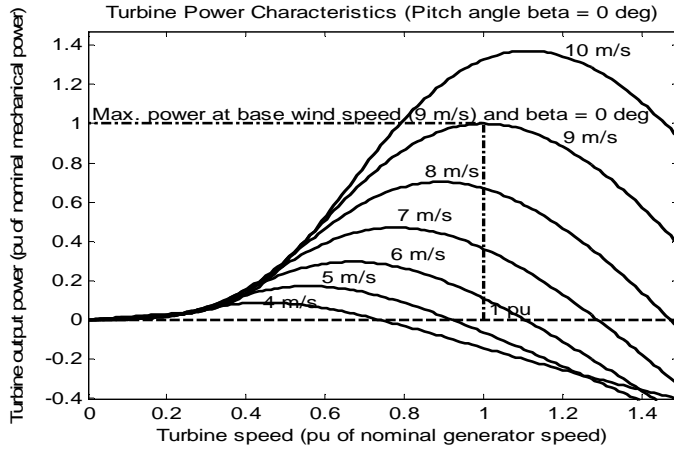


Fig. (1) Power as a function of rotor speed for different wind speeds.

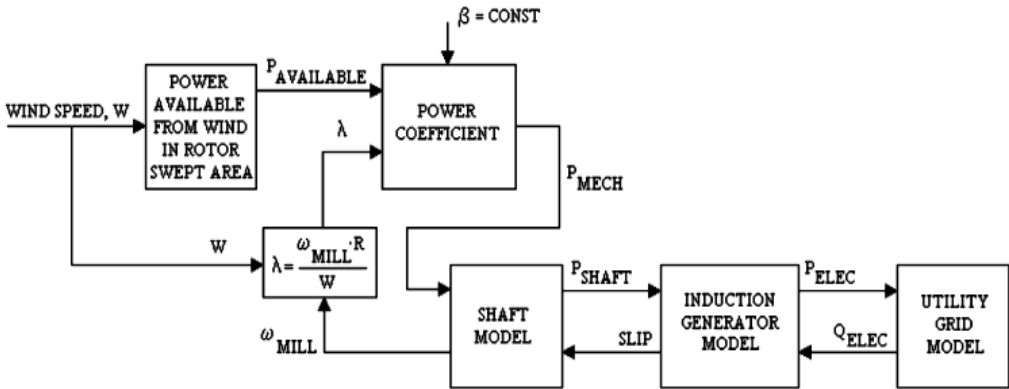


Fig. (2) Modular model of a grid-connected, stall-controlled wind turbine equipped with an IG

2.2 Induction Generator Model

The electrical part of the machine is represented by a second-order state-space model and the mechanical part by a second-order system. All electrical variables and parameters are referred to the stator. All stator and rotor quantities are in the arbitrary two-axis reference frame (d-q frame). The d-axis and q-axis block diagram of the electrical system is shown in Fig. (3). The electrical equations are given by:

$$V_{qs} = R_s i_{qs} + \frac{d}{dt} \phi_{qs} + \omega \phi_{ds} \tag{5}$$

$$V_{ds} = R_s i_{ds} + \frac{d}{dt} \phi_{ds} - \omega \phi_{qs} \tag{6}$$

$$V'_{qr} = R'_r i_{qr} + \frac{d}{dt} \phi'_{qr} + (\omega - \omega_r) \phi'_{dr} \tag{7}$$

$$V'_{dr} = R'_r i_{dr} + \frac{d}{dt} \phi'_{dr} - (\omega - \omega_r) \phi'_{qr} \tag{8}$$

$$T_e = 1.5 p (\phi_{ds} i_{qs} - \phi_{qs} i_{ds}) \tag{9}$$

Where: $\phi_{qs} = L_s i_{qs} + L_m i'_{qr}$, $\phi_{ds} = L_s i_{ds} + L_m i'_{dr}$, $\phi'_{qr} = L'_r i'_{qr} + L_m i_{qs}$,
 $\phi'_{dr} = L'_r i'_{dr} + L_m i_{ds}$

With: $L_s = L_{ls} + L_m$ and $L'_r = L'_{lr} + L_m$

The mechanical equations are given by:

$$\frac{d}{dt} \omega_m = \frac{1}{2H} (T_e - F \omega_m - T_m) \tag{10}$$

$$\frac{d}{dt} \theta_m = \omega_m \tag{11}$$

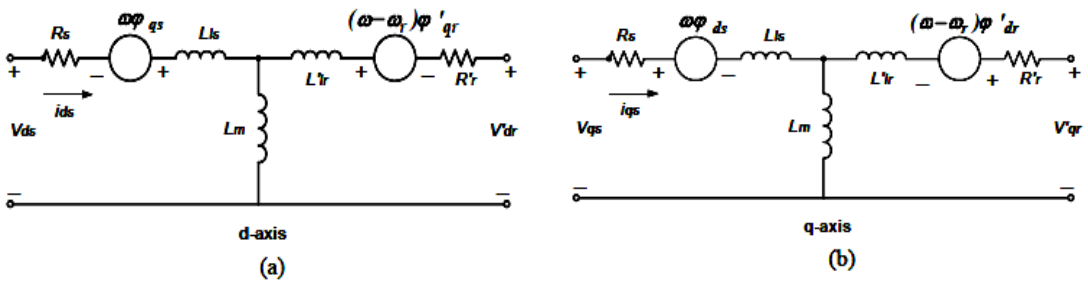


Fig. (3) Induction machine equivalent circuits
 (a) d-axis equivalent circuit (b) q-axis equivalent circuit

2.3 Wind Turbine Induction Generator WTIG

The block diagram of WTIG is shown in Fig. (4), and the stator winding is connected directly to the 60 Hz grid and the rotor is driven by a variable pitch wind turbine. The power captured by the wind turbine is converted into electrical power by the induction generator and is transmitted to the grid by the stator winding. The pitch angle is controlled in order to limit the generator output power to its nominal value for high wind speeds. In order to generate power the induction generator speed must be slightly above the synchronous speed. The pitch angle controller regulates the wind turbine blade pitch angle β , according to the wind speed variations. Hence, the power output of WTIG depends on the characteristics of the pitch controller in addition to the turbine and generator characteristics.

This control guarantees that, irrespective of the voltage, the power output of the WTIG for any wind speed will be equal to the designed value for that speed. The pitch angle β is controlled in order to limit the generator output power at its nominal value for winds exceeding the nominal speed. β is controlled by a Proportional-Integral PI controller in order to limit the electric output power to the nominal mechanical power. When the measured electric output power is under its nominal value, β is kept constant at zero degree. When it increases above its nominal value the PI controller increases β to bring back the measured power to its nominal value. The pitch angle control system is shown in Fig. (5). In order to generate power, the IG speed must be

slightly above the synchronous speed. Speed varies approximately between 1.0 pu at no load and 1.005 pu at full load.

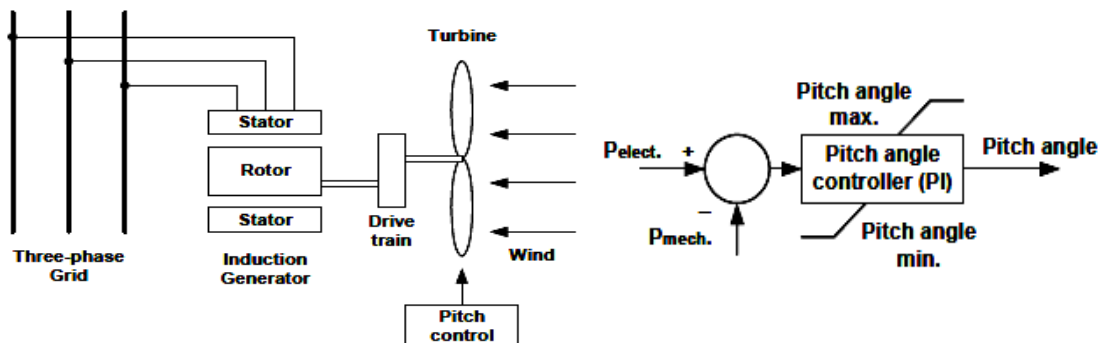


Fig. (4) Block diagram of WTIG Fig. (5) Control system for pitch angle control

2.4 Protection System

Commercial wind turbines incorporate sophisticated system for protection of electrical and mechanical components. These turbine-based protection systems respond to local conditions, detecting grid or mechanical anomalies that indicate system trouble or potentially damaging conditions for the turbine. The protection system should respond almost instantaneously to mechanical speed, vibration, voltages, or currents outside of defined tolerances. In addition, conventional multi-function relays for electric machine protection should also be provided to detect a wide variety of grid disturbances and abnormal conditions within the machine. In the present study, the WTIG protection system consists of the followings: Instantaneous/positive-sequence AC Overcurrent, AC Current Unbalance, AC Overvoltage/Undervoltage (positive-sequence), AC Voltage Unbalance (Negative-sequence / Zero sequence) and DC Over voltage.

2.5 SVC Modeling

SVC is a first generation FACTS device, can control voltage at the required bus thereby improving the voltage profile of the system. The primary task of an SVC is to maintain the voltage at a particular bus by means of reactive power compensation. SVCs have been used for high performance steady state and transient voltage control compared with classical shunt compensation. SVCs are also used to dampen power swings, improve transient stability, and reduce system losses by optimized reactive power control [24]. SVC is basically a shunt connected Static Var Generator SVG whose output is adjusted to exchange capacitive or inductive current so as to maintain or control specific power system variables. Figure (6) shows the single-line diagram of a SVC and a simplified block diagram of its control system [16]. A typically, the power system control variable controlled by SVC is the terminal bus voltage, and total susceptance of SVC can be controlled by firing thyristors. Consequently, it represents the controller with variable impedance that is changed with the firing angle of TCR. The terminal or $V-I$ characteristics of SVC is illustrated in Fig. (7).

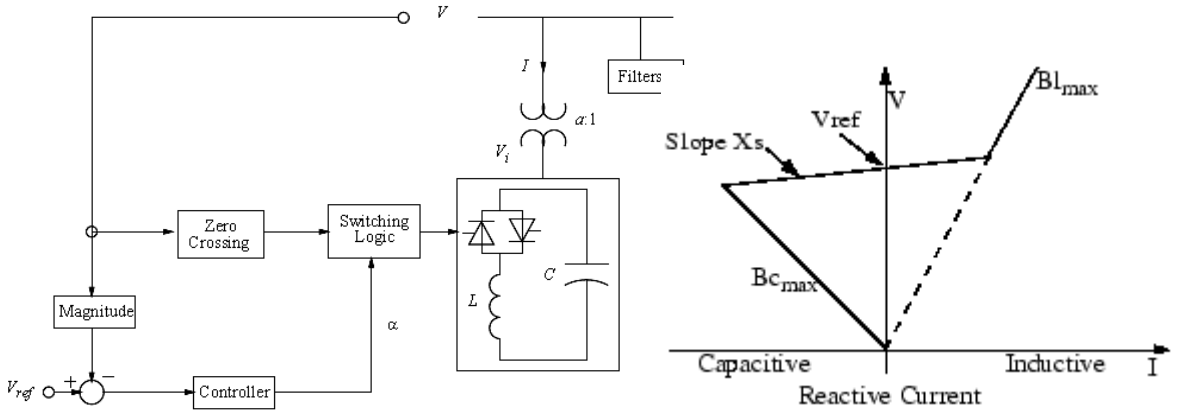


Fig. (6) Basic SVC structure with voltage control system Fig. (7) V-I characteristics of a SVC

SVC can immediately provide reactive power support when the system has voltage problem due to a trip of an important generator or transmission line. In some applications, it can be used as an aid to improve stability; SVC can perform the duty of providing rapidly controlled vars more appropriately during the first angle swing and thus, by maintaining the voltage, inherently improve transient stability. In addition, it is possible with a SVC not only to maintain a reference voltage level, but also to modulate the reference voltage signal in order to improve system damping [25]. The validated p.u. Differential-Algebraic Equations (DAEs) corresponding to this model are [26]:

$$\begin{bmatrix} \dot{x}_c \\ \dot{\alpha} \end{bmatrix} = f(x_c, \alpha, V, V_{ref}) \quad (12)$$

$$0 = \underbrace{\begin{bmatrix} B_{SVC} - \frac{2\alpha - \sin 2\alpha - \pi(2 - X_L / X_C)}{\pi X_L} \\ I - V_i B_{SVC} \\ Q - V_i^2 B_{SVC} \end{bmatrix}}_{g(\alpha, V, V_i, I, Q, B_{SVC})} \quad (13)$$

The differential equations represented by equation (12) vary with the type of control system used. Figure (8) depicts a typical voltage control block diagram, which includes a droop to avoid continuous operation of the controller and to allow for proper coordination with other voltage controllers in the network. It is important to highlight the fact that an admittance model is numerically more stable than the corresponding impedance model, i.e., using B_{SVC} on the model averts numerical problems when close to the controller's resonant points [27]. The bias α_o for this controller is determined by solving the equations resulting from forcing $B_{SVC}=0$ in equation (13), i.e., this value corresponds to the resonant point of the SVC ($I = 0$) and is obtained by solving the nonlinear equation:

$$2\alpha_o - \sin 2\alpha_o - \pi(2 - X_L / X_C) = 0 \quad (14)$$

where, X_C and $f(\cdot)$ stand for the control system variables and equations, respectively. These equations represent limits not only on the firing angle α , but also on the current I , the control voltage V and the SVC voltage V_i as well as the reactive power. The SVC steady state model can be obtained by replacing the equations (12) and (13) with:

$$0 = \begin{bmatrix} V - V_{ref} - X_{SL} I \\ g(\alpha, V, V_i, I, Q, B_{SVC}) \end{bmatrix} \quad (15)$$

Which can be directly included in any power flow program with the proper handling of firing angle limits. Note that equation (13) provides the relationship between SVC susceptance B_{SVC} and α , I and Q .

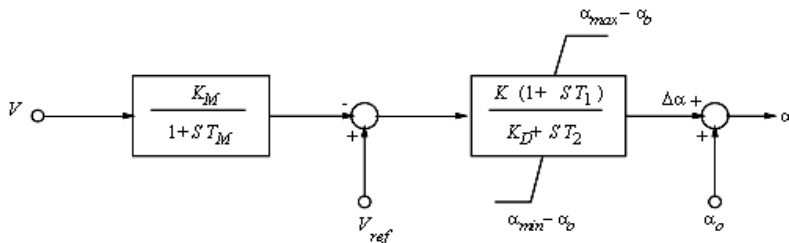


Fig. (8) SVC control block diagram

2.6 STATCOM Modeling

There are two techniques for controlling the STATCOM. The first technique, referred to as phase control, is to control the phase shift β to control the STATCOM output voltage magnitude. The other technique referred to as Pulse Width Modulation (PWM) on the other hand allow for independent control of output voltage magnitude and phase shift, in this case, the dc voltage is controlled separately from the ac output voltage. The basic structure of a STATCOM with PWM-based voltage controls is depicted in Fig. (9) [27-29]. Eliminating the dc voltage control loop on this figure would yield the basic block diagram of a controller with a typical phase angle control strategy. PWM controls are becoming a more practical option for transmission system applications of VSC-based controllers, due to some recent developments on power electronic switches that do not present the high switching losses of GTOs [30], which have typically restricted the use of this type of control technique to relatively low voltage applications. In PWM controls, switching losses associated with the relatively fast switching of the electronic devices and their snubbers play an important role in the simulation, as these have a direct effect on the charging and discharging of the capacitor, and hence should be considered in the modeling.

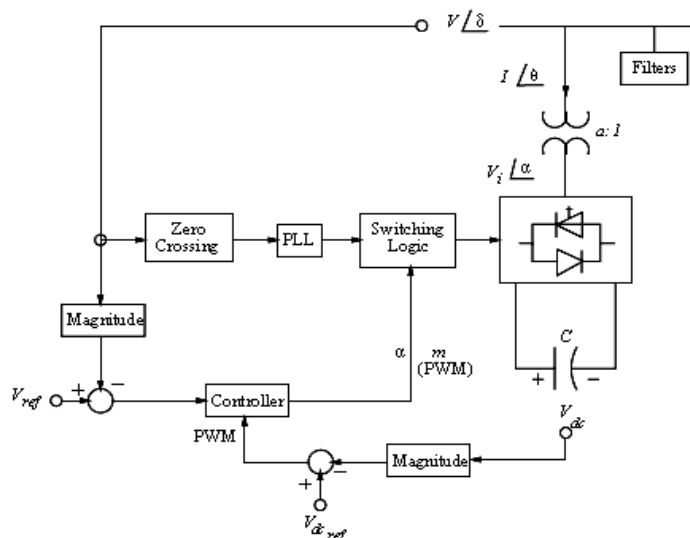


Fig. (9) Block diagram of a STATCOM with PWM voltage control

By varying the amplitude of output voltage can control the reactive power exchange between the inverter and the ac system. If the amplitude of the output voltage is increased above that of ac system voltage, the inverter generates reactive power for the ac system. If the amplitude of the output voltage is decreased below that of the ac system, the inverter absorbs the reactive power. If the output voltage is equal to the ac system voltage, the reactive power exchange is zero. Conversely, the inverter absorbs real power from the ac system, if the inverter output voltage is made to lag the ac system voltage. The V-I characteristic of STATCOM controller is shown in Fig. (10), the controller can provide both capacitive and inductive compensation and is able to control output current over the rated maximum capacitive or inductive range independent of the ac system voltage. It can provide full capacitive output current at any practical system voltage. This is in contrast to the SVC which can supply only a diminishing output current with decreasing system voltage as determined by the designed maximum equivalent capacitive admittance. This type of controller is, therefore, more effective than the SVC in providing transmission voltage support and the expected stability improvements. In general, a reduction of more than 50% in the physical size of installation can be expected from STATCOM compared to SVC.

Also, for steady state reactive support, a STATCOM is capable of supporting higher loads than what would be possible with a SVC of comparable MVAR rating. The STATCOM may have an increased transient rating in both the inductive and capacitive operating regions, which can further enhance its dynamic performance. The SVC can increase transient var absorption capability only. The transient rating of the STATCOM is dependent on the characteristics of the power semiconductors used and the maximum junction temperature at which the devices can be operated. Assuming balanced, fundamental frequency voltages, the controller can be accurately represented in transient stability studies using the basic model as shown in Fig. (11) [30]. STATCOM should be modeled to cover the limits in both control and operation.

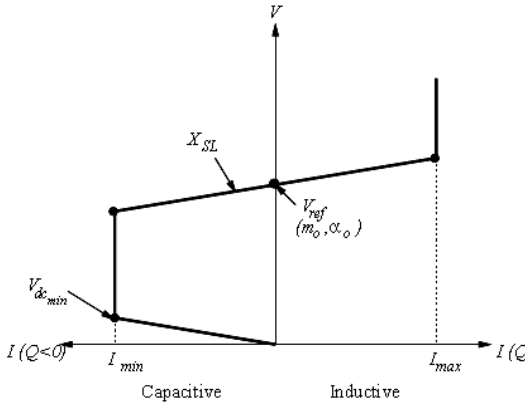


Fig. (10) V-I characteristics of a STATCOM

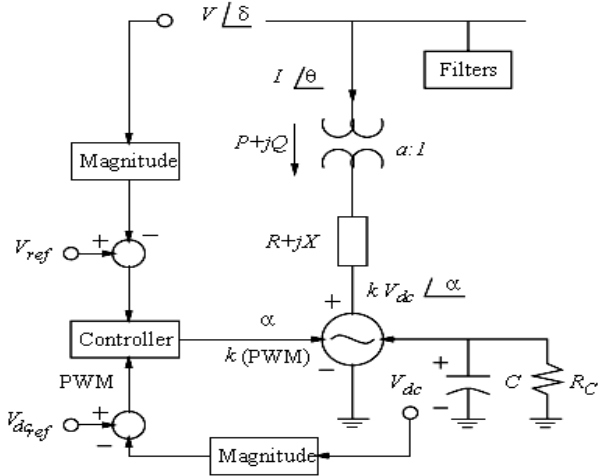


Fig. (11) Transient stability model of a STATCOM with PWM voltage control

Instead of representing STATCOM by a synchronous machine as in the conventional method, the appropriate models of the controller should be used to have a more accurate result. To fulfill that, the p.u. Differential-Algebraic Equations (DAEs) corresponding to this model are described as follows [26]:

$$\begin{bmatrix} \dot{x}_c \\ \dot{\alpha} \\ \dot{m} \end{bmatrix} = f(x_c, \alpha, m, V, V_{dc}, V_{ref}, V_{dc,ref}) \tag{16}$$

$$\dot{V}_{dc} = \frac{VI}{CV_{dc}} \cos(\delta - \theta) - \frac{1}{R_c C} V_{dc} - \frac{R}{C} \frac{I^2}{V_{dc}} \tag{17}$$

$$0 = \underbrace{\begin{bmatrix} P - VI \cos(\delta - \theta) \\ Q - VI \sin(\delta - \theta) \\ P - V^2 G + kV_{dc} VG \cos(\delta - \alpha) + kV_{dc} VB \sin(\delta - \alpha) \\ Q + V^2 B - kV_{dc} VB \cos(\delta - \alpha) + kV_{dc} VG \sin(\delta - \alpha) \end{bmatrix}}_{g(\alpha, k, V, V_{dc}, \delta, I, \theta, P, Q)} \tag{18}$$

where most of the variables are explained on Fig. (11), The variables x_c and functions $f(\cdot)$ in equation (16) stand for the internal control system variables and equations, respectively, and hence vary depending on whether a PWM or phase control technique is used in the controller. The admittance $G + jB = (R + jX)^{-1}$ is used to represent the transformer impedance and any ac series filters (e.g. smoothing reactors), the constant $k = \sqrt{3/8}m$ is directly proportional to the modulation index m . A simple PWM voltage controller is shown in Fig. (12) [28, 31], which basically defines the differential equations represented by $f(\cdot)$ in equation (16). Observe that the ac bus voltage

magnitude is controlled through the modulation index m , since this has a direct effect on the ac side of VSC voltage magnitude. Whereas the phase angle, α , which basically determines the active power P flowing into the controller is used to directly control the dc voltage magnitude since the power flowing into the controller charges and discharges the capacitor.

The controller limits are defined in terms of the controller current limits, which are directly related to the switching device current limits, as these are the basic limiting factor in VSC-based controllers. In simulations, these limits can be directly defined in terms of the maximum and minimum converter currents I_{max} and I_{min} , respectively, i.e., the integrator blocks are "stopped" whenever the converter current I reaches a limit, which would allow to closely duplicate the steady state V-I characteristics of the controller shown in Fig. (10). Another option is to compute these limits by solving the steady state equations of the converter; these equations are also used to compute the biases m_o and α_o [32].

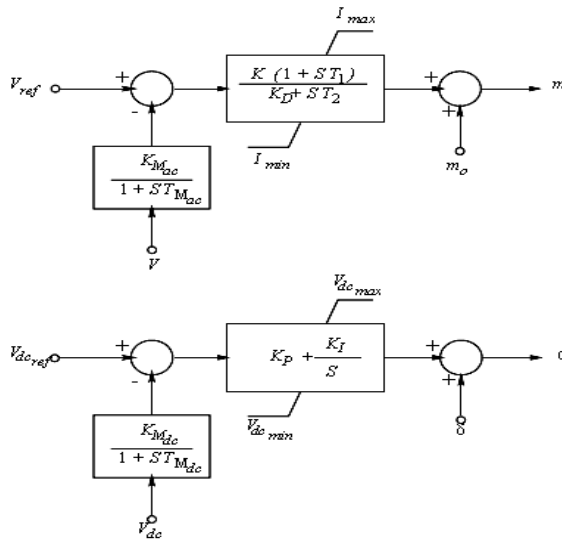


Fig. (12) Basic STATCOM PWM voltage control

The steady state model can be readily obtained from equations (16)-(18) by replacing the differential equations with the steady state equations of the dc voltage and the voltage control characteristics of the STATCOM:

$$0 = \begin{bmatrix} V - V_{ref} \pm X_{SL} I \\ V_{dc} - V_{dcref} \\ P - V_{dc}^2 / R_C - RI^2 \\ g(\alpha, k, V, V_{dc}, \delta, I, \theta, P, Q) \end{bmatrix} \tag{19}$$

2.7 Studied System

The one line diagram of the test system employed in this study is shown in Fig. (13). The network consists of a 120-kV, 60-Hz, sub-transmission system with short circuit level of 2500 MVA, feeds a 25 kV distribution system through 120/25kV step down transformers.

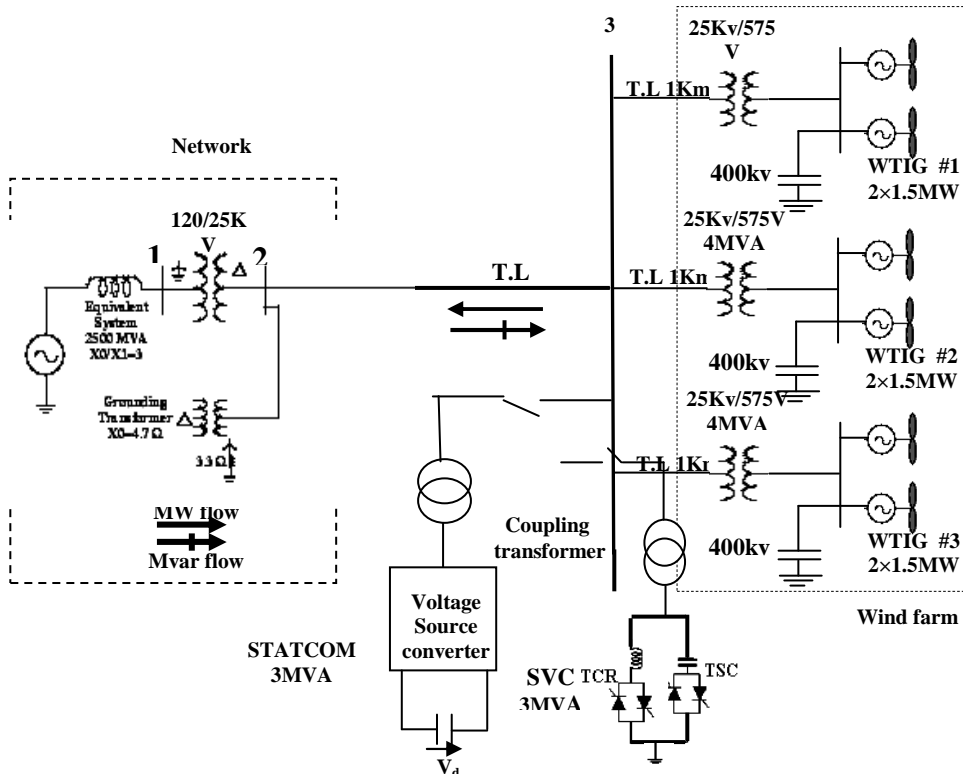


Fig. (13) Single-line diagram of the distribution system embedded with WTIG and FACTS devices

A wind farm consisting of 1.5-MW wind turbines and driven squirrel-cage induction generator is connected to the 25-kV distribution system, exports power to the 120-kV grid through a 25-km 25-kV feeder. Part of the reactive power consumed by the induction generators is locally supplied by fixed capacitors of 400 Kvar each, installed at the terminals of the machines. Dynamic reactive power compensation is provided by a 3MVA STATCOM and 3 MVA SVC. In order to limit the generator output power at its nominal value, the pitch angle is controlled for winds exceeding the nominal speed of 9 m/s. To inject active power to the distribution network, the IG speed must be slightly above the synchronous speed. Speed varies approximately between 1.0 pu at no load and 1.005 pu at full load. Each wind turbine has a protection system, monitoring voltage, current and machine speed. The amount of active power injected by WTIGs to the distribution system is limited by transient stability issues [11, 32].

3. RESULTS AND DISCUSSIONS

It's intended to improve the wind farm power system performance while the studied system is subjected to many types of disturbances. The first disturbance is the change in wind speed on wind turbines, and phase-to-phase ground fault occurred at terminals of WTIG #2 cleared after 100 ms is second disturbance. Further, three phase to ground fault occurred at bus #3 and was cleared after 100 ms is applied, Sudden injection and

rejection loads at $t=15\text{sec}$ is occurred. The fifth disturbance is an inserting of composed load plant consisting of motor load and resistive load. The effects of combination between SVC and STATCOM on the system parameters performance are studied. The power system performance due to the above disturbance can be examined as follows:

3.1 Effect of the wind speed change disturbance:

The wind speed changes for each turbine are as follows: initially, wind speed is set at 8m/s , disturbance starts at $t=2\text{s}$ by raising linearly the speed to 11m/s for WTIG #1. The same gust of wind is applied to WTIG #2 and WTIG #3, respectively with at $t=4\text{sec}$ and $t=6\text{sec}$ respectively as shown in Fig. (14). Without the use of any FACTS device, WTIG #1 is tripped at $t=13.43\text{sec}$ while WTIG #2 and WTIG#3 are still working so the active power generated from each WTIG is 3MW with absorbing reactive power is 1.47Mvar , also the turbine speed response for WTIG #1 is highly increased. With the use of SVC only or STATCOM only or the combination in between, the three WTIG are still working so the WTIG output active power generated from each WTIG is 3MW , the reactive power absorbed with each WTIG is 1.47Mvar . Fig. (14) illustrates the total absorbed reactive power from the network and the voltage bus #3, it's noted that the total absorbed reactive power is decreased in the case of a combination between SVC and STATCOM, also voltage at bus #3 is improved.

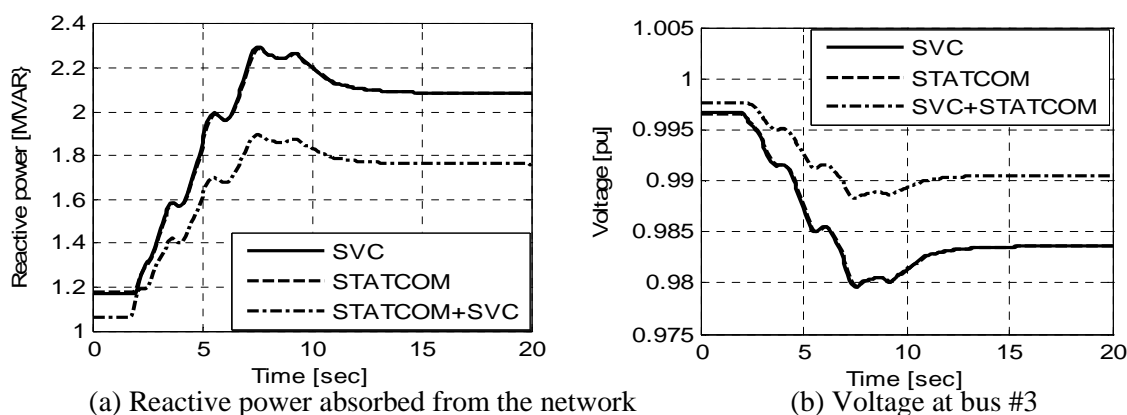
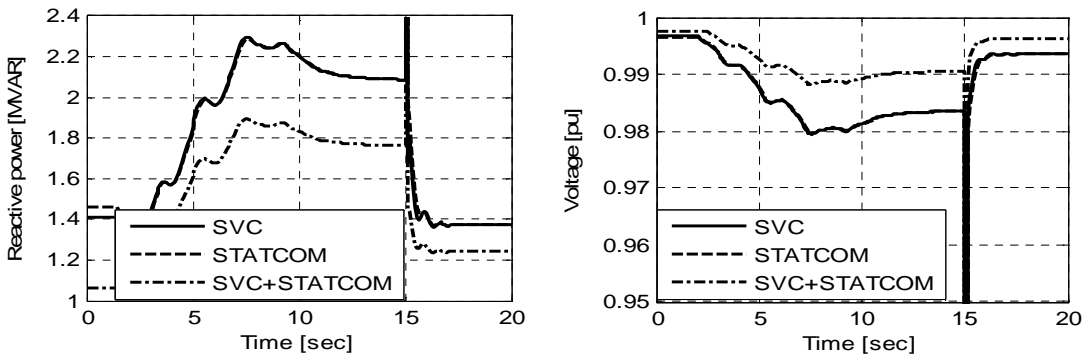


Fig. (14) Effects of the wind speed change on bus #3 parameters

3.2 Effect of phase-to-phase ground fault on terminal WTIG #2:

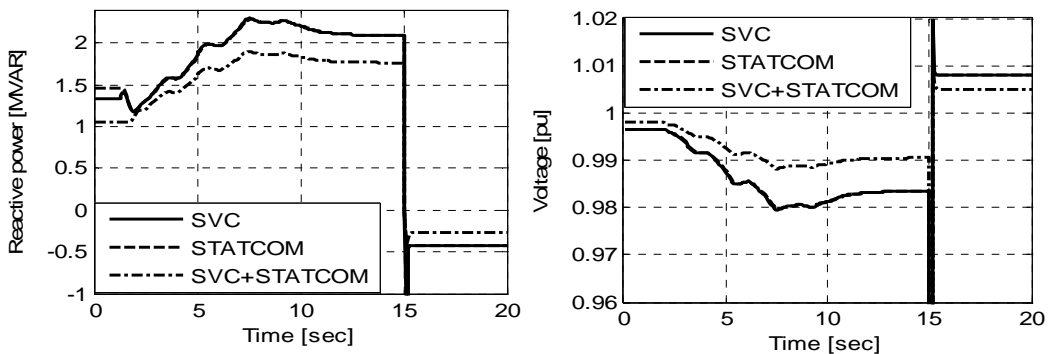
Figure (15) show the change in wind speed and the studied system is subjected to phase-to-phase ground fault occurred on terminal WTIG #2 only and is cleared after 100ms from 15sec to 15.1sec . Without the use of any FACTS device, the WTIG # 1 is tripped at $t=13.43\text{sec}$ and the WTIG # 2 is tripped at $t=15.11\text{sec}$ but WTIG #3 is still working to generate 3MW . But when we use FACTS devices such as SVC of (3MVA) rating or STATCOM of (3MVA) rating or the combination between SVC & STATCOM connected at bus #3, WTIG # 2 only is tripped at $t=15.11\text{sec}$, but WTIG #1 and WTIG #3 are still working. The total absorbed reactive power from the network and the voltage bus #3 responses are depicted in Fig. (15). It's noted that the total absorbed reactive power is decreased in case the of a combination between SVC and STATCOM, also the voltage at bus #3 is improved.



(a) Reactive power absorbed from the network (b) Voltage at bus #3
 Fig. (15) Effects of phase-to-phase to ground on bus #3 parameters

3.3 Effect of a three phase ground fault on bus #3:

The impact of change in wind speed and the studied system subjected to three phase to ground fault occurred on bus #3 and cleared after 100ms from 15sec to 15.1sec is studied. Without use of the FACTS devices, WTIG #1 is tripped at $t=13.43\text{sec}$ and WTIG #2 & WTIG #3 are tripped $t=15.1\text{sec}$ by the protection system. Despite of the presence of each SVC of (3MVA) or STATCOM of (3MVA) or both, but three WTIG are tripped because of insufficiency capacity of SVC & STATCOM to supply necessary reactive power. Figure (16) shows the reactive power absorbed from the network, during fault at $t=15\text{sec}$, the reactive power absorbed from the network decreases reach to zero. After fault clearing at $t=15.1\text{sec}$, it decreases to -0.428Mvar with the presence of SVC or STATCOM and increase to -0.2626Mvar with the presence of SVC & STATCOM, also the voltage on bus #3, during fault $t=15\text{sec}$ decrease reach to zero. After fault clearing at $t=15.1\text{sec}$, it increases to reach 1.008pu with the presence of SVC only or STATCOM only and increases to reach 1.005pu with the presence of SVC & STATCOM.

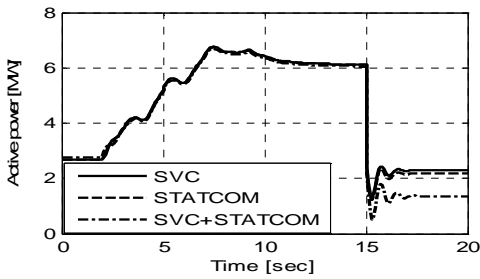


(a) Reactive power absorbed from the network (b) Voltage at bus #3
 Fig. (16) Effects of a three-phase ground at bus #3 on bus #3 parameters

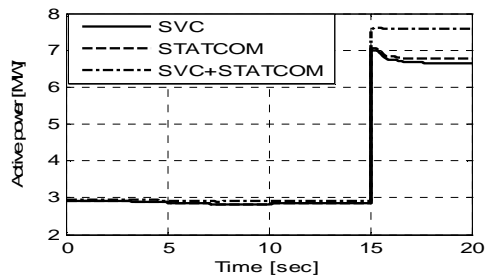
3.4 Effect of sudden injection of loads on bus #3:

The impact of a change in wind speed and a connection of an inductive load of (5MW+J2Mvar) on bus #3 at $t=15\text{sec}$ plus an inductive load of (3MW+J2Mvar)

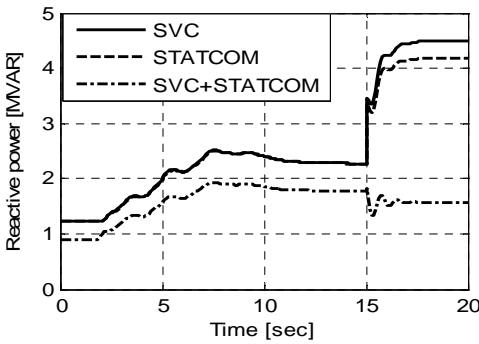
initially connected are studied. Figure (17) illustrates the total active power injected to the network, the total absorbed reactive power from the network and the voltage bus#3 responses with SVC only, STATCOM only and a combination in between due to sudden injection load disturbance on bus #3. It's noted that the combination between SVC and STATCOM connection causes the required active power load can be provided from wind farm. Further, the combination between SVC and STATCOM gives less overshoot in reactive power response and decreases reactive power absorbed from the network. Moreover, the voltage at bus #3 improves. The total load active power, the total load reactive power and voltage at bus #3 responses with combination between SVC and STATCOM due to sudden injection load are shown in Fig. (18). It's noted that the bus voltage improve whereupon the active power injected to load increases as shown Fig. (18).



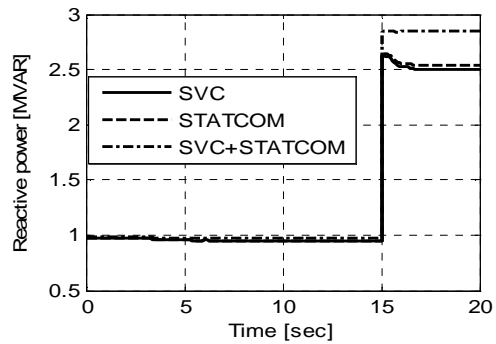
(a) Active power injection to the network



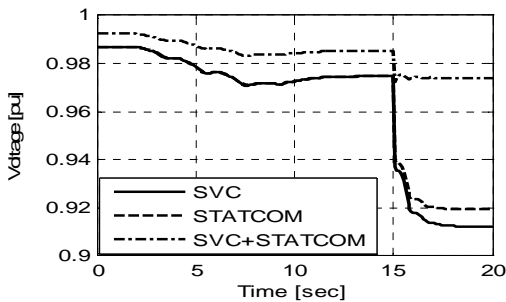
(a) Active power injection to Load



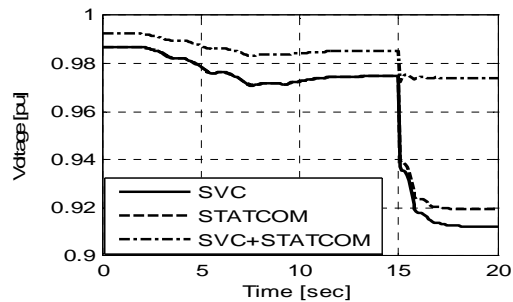
(b) Reactive power absorbed from the network



(b) Reactive power injection to Load



(c) Voltage at bus #3



(c) Load Voltage

Fig. (17) Effect of the injection of a load on bus #3

Fig. (18) Effect of injection of a load on the load

load increases as shown Fig. (18).

3.5 Effect of a sudden rejection of a load on bus #3:

The impact of change in wind speed and rejection of an inductive load of (5MW+J2Mvar) on bus #3 at t=15sec is studied as shown in Fig. (19). Figure (20) illustrates the total active power injected to the network, the total absorbed reactive power from the network and the voltage at bus #3 responses with SVC only, STATCOM only and the combination in between due to a sudden rejection of the load disturbance on bus #3. It's noted that the combination between SVC and STATCOM connection causes that the required active power load can be provided from the wind farm. Further, the combination between SVC and STATCOM gives less overshoot in reactive power response and decreases the reactive power absorbed from the network. Moreover, the voltage at bus #3 improves as shown in Fig. (21). The total load active power, the total load reactive power and the voltage at bus #3 responses with the combination between SVC and STATCOM due to sudden rejection load are shown in Fig. (21). It's noted that the bus voltage improves whereupon they active power injected to load.

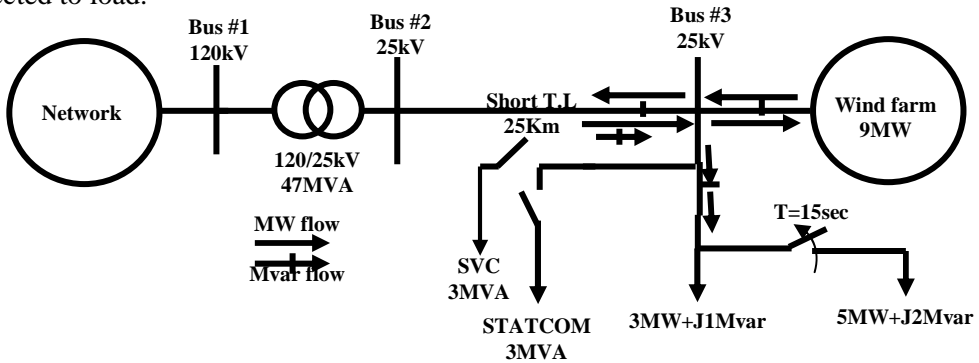
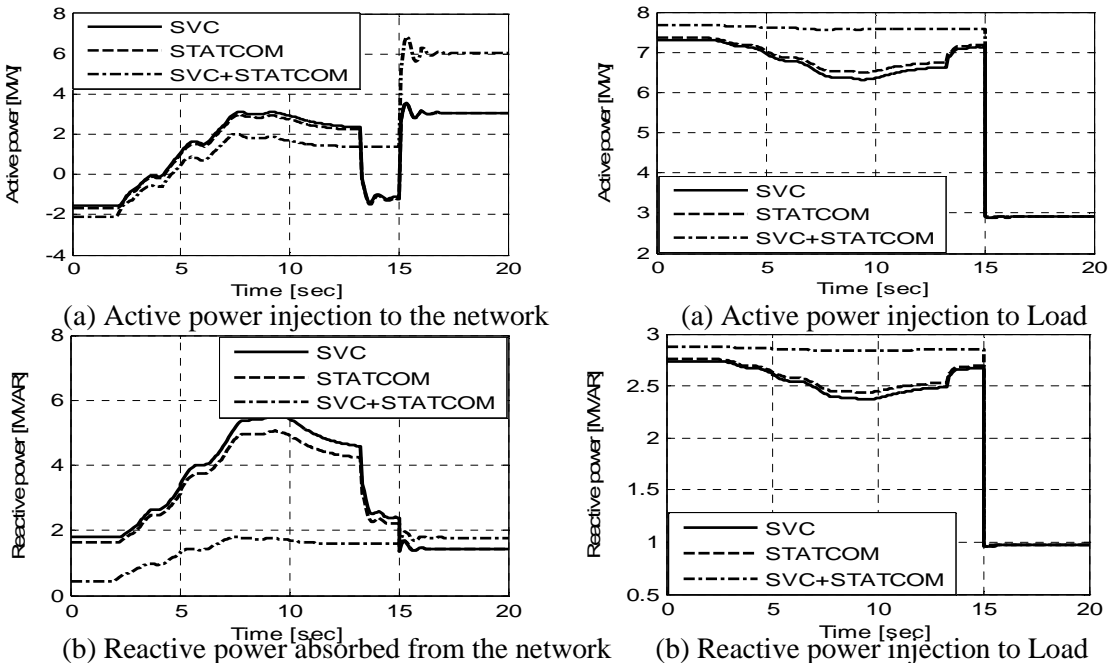
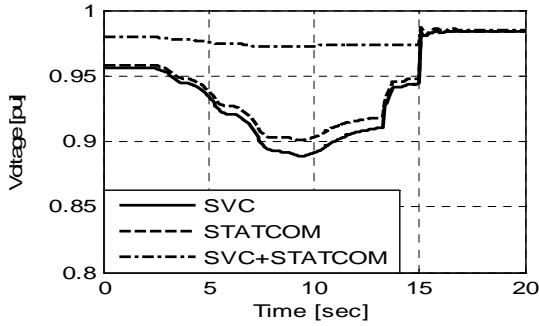
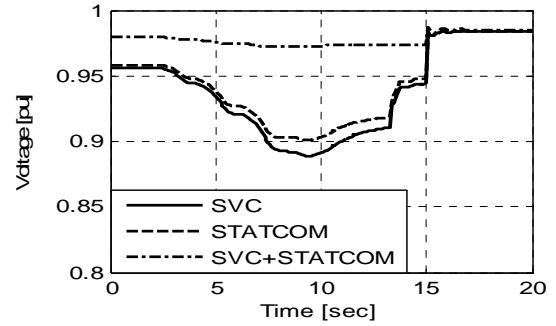


Fig. (19) Line diagram of the distribution system embedded with WTIG, FACTS and inductive loads





(c) Voltage at bus #3



(c) Load Voltage

Fig. (20) Effects of rejection load on bus #3

Fig. (21) Effects of rejection load on loads parameters

3.6 Effect of the connection of a plant

The impact of the change in wind speed and the connection of a plant consisting of an induction motor and resistive load is shown in Fig. (22). Figure (23) illustrates the total active power injected to the network, the total absorbed reactive power from the network and the voltage at bus #3 responses with the presence of SVC only, STATCOM only and the combination between SVC & STATCOM. It is noted that the reactive power absorbed from the network decreases and the voltage at bus improves with the presence of the combination of SVC & STATCOM. The total plant active power, the total plant reactive power and the plant voltage responses with presence of SVC only, STATCOM only and the combination between SVC & STATCOM due to connection of a plant are shown in Fig. (24). It's noted that the combination SVC & STATCOM improves the bus voltage whereupon the active power injected to load increases.

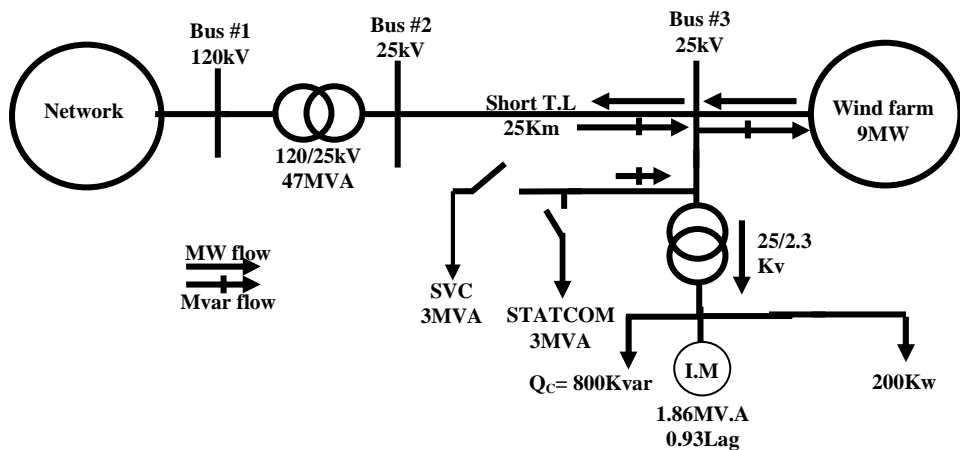
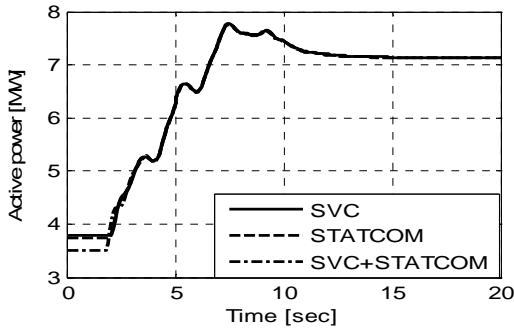
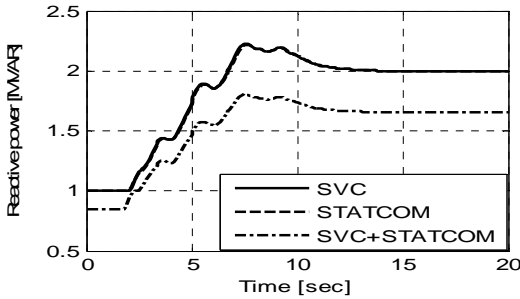


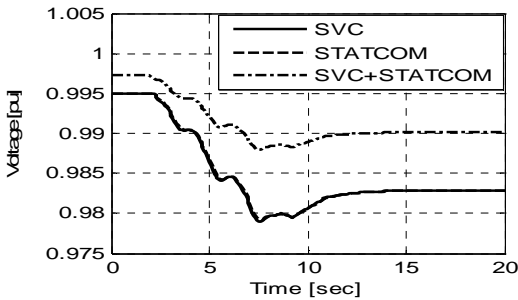
Fig. (22) Line diagram of the distribution system embedded with WTIG, STATCOM and plant



(a) Active power injection to the network

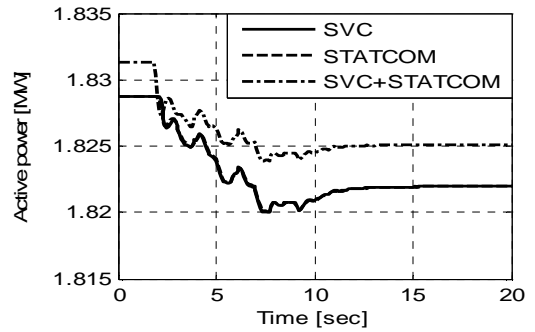


(b) Reactive power absorbed from the network

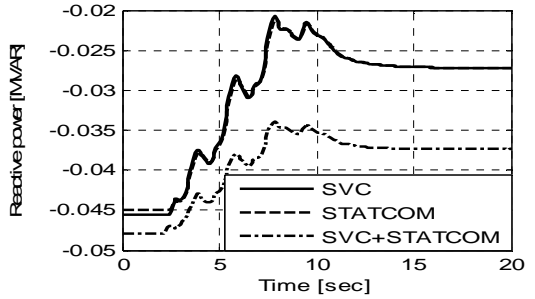


(c) Voltage at bus #3

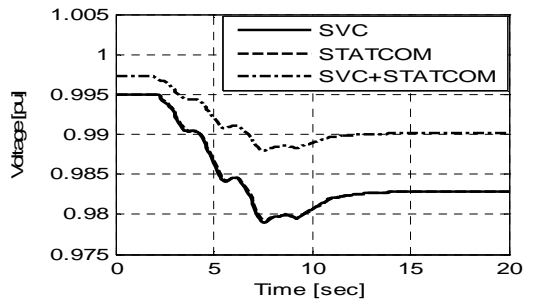
Fig. (23) Effects of the connection of a Plant on bus #3 parameter



(a) Active power injection to Plant



(b) Reactive power injection to Load



(c) Load Voltage

Fig. (24) Effects of the connection of a Plant on Plant parameter

4. CONCLUSIONS

The effect of connecting a combined SVC & STATCOM on wind farm power system variables is studied. Active power injected to the network, reactive power absorbed from the network, turbine speed and bus voltage at bus #3 due to different disturbance applied to the system can be summarized as follows:

- At a change of the wind speed from 8m/sec to 11m/sec, without using FACTS devices, WTIG #1 is tripped at $t=13.43\text{sec}$ so the active power injected to the network is 6MW. While, a combination from SVC & STATCOM is better than the use of SVC only or the use of STATCOM only in terms of improving the voltage at bus #3 to reach 0.99pu and reducing the absorbed reactive power to 1.76MVAR.

- Due to the occurrence of a phase to phase ground fault on terminal WTIG #2 at $t=15\text{sec}$ with the presence of a change in wind speed from 8m/sec to 11m/sec , without the using of FACTS devices, WTIG #1 and WTIG #2 are tripped at $t=13.4\text{sec}$, $t=15.11\text{sec}$ respectively, so the active power injected to the network is 3MW . While, a combined SVC & STATCOM is better than using only SVC or using only STATCOM in sense of improving the voltage during fault at bus #3 to reach 0.75pu and reducing the absorbed reactive power to 6.65Mvar
- Assume the occurrence of a three phase to ground fault on bus #3 at $t=15\text{sec}$ with the presence of a change in wind speed from 8m/sec to 11m/sec . The three WTIG are tripped, so the active power injected to the network is zero. With the presence of only SVC or only STATCOM or combined SVC & STATCOM the three WTIG are tripped at $t=15.11\text{sec}$, so the active power injected to the network is zero.
- At a sudden injection of an inductive load ($5\text{MW}+j2\text{Mvar}$) at $t=15\text{sec}$ plus an initial inductive load ($3\text{MW}+j2\text{Mvar}$) with the presence of a change in wind speed and without using FACTS devices, the WTIG #1 is tripped, so the active power injected to the network is -0.2MW . While, with the presence only of SVC or only STATCOM or combined SVC & STATCOM, three WTIG are still working.
- At the sudden rejection of an inductive load ($5\text{MW}+j2\text{Mvar}$) at $t=15\text{sec}$ from total load ($8\text{MW}+j3\text{Mvar}$) with the presence of a change in wind speed, without using FACTS devices, the WTIG #1 and the WTIG #2 are tripped at $t=13.29\text{sec}$ and $t=7.127\text{sec}$ respectively so the active power injected to the network is 0.14MW . While, with the presence of only STATCOM or only SVC, the WTIG #1 only is tripped at $t=13.29\text{sec}$ and then the rejection of a load disturbance is applied at $t=15\text{sec}$, but with the presence of a combination of a SVC & STATCOM, three WTIG are still working.
- Assume a connection of a plant consisting of induction motor and resistive load with the presence of change in wind speed, without the use of FACTS devices, the WTIG #1 is tripped at $t=13.39\text{sec}$ so the active power injected to the network is 4.15MW . While, with the presence of SVC only or STATCOM only or the combination from SVC & STATCOM, three WTIG are still working.
- From the simulation results, a combination from SVC and STATCOM gives better performance as compared to using SVC only or using STATCOM only and only STATCOM has better performance as compared to the use of SVC only in case of heavy load.

REFERENCES

- [1] J.F. Manwell, J.G. McGowan and A.L. Rogers, "Wind Energy Explained – Theory, Design and Application", John Wiley & Sons, ch. 7, 2002.
- [2] Tony Burton, David Sharpe, Nick Jenkins and Ervin Bossanyi, "Wind Energy Handbook", John Wiley & Sons, ch. 4, 2001.
- [3] Eduard Muljadi and C. P. Butterfield, "Pitch-Controlled Variable-Speed Wind Turbine Generation", IEEE Transactions on Industry Applications, vol. 37, no. 1, pp. 240-246, 2001.

- [4] B. Ted, "A Novel Control Scheme for a Doubly-Fed Induction Wind Generator under Unbalanced Grid Voltage Conditions", CEME Tele seminar, 2007
- [5] E. Muljadi, C.P. Butterfield, J. Chacon, H. Romanowitz, "Power Quality Aspects in a Wind Power Plant", IEEE Power Engineering Society General Meeting, 2006
- [6] A. Vladislav, "Analysis of Dynamic Behavior of Electric Power Systems with Large Amount of Wind Power", a dissertation submitted to Electric Power Engineering, Technical University of Denmark, Denmark, 2003
- [7] Heping Zou, Hui Sun, Jiyan Zou, "Fault Ride-through Performance of Wind Turbine with Doubly Fed Induction Generator", 2nd IEEE Conference on Industrial Electronics and Applications, pp. 1607-1611, 2007.
- [8] F. Jurado and J. Carpio, "Enhancing the Distribution Networks Stability using Distributed Generation", The International Journal for Computation and Mathematics in Electrical and Electronic Engineering, vol. 24, no. 1, pp. 107-126, 2005.
- [9] Vijay Vittal, "Consequence and Impact of Electric Utility Industry Restructuring on Transient Stability and Small-Signal Stability Analysis", IEEE Proceedings, vol. 88, no. 2, pp. 196-207, 2000.
- [10] O. Samuelsson and S. Lindahl, "On Speed Stability", IEEE Trans. Power Sys., vol. 20, no. 2, pp. 1179 – 1180, 2005.
- [11] N. D. Hatziaargyriou and A. P. S. Meliopoulos, "Distributed Energy Sources Technical Challenges", IEEE Power Engineering Society Winter Meeting, vol. 2, pp. 1017 – 1022, 2002.
- [12] R. Gnativ and J. V. Milanovi, "Voltage Sag Propagation in Systems with Embedded Generation and Induction Motors", IEEE Power Engineering Society Summer Meeting, vol. 1, pp. 474 – 479, 2001.
- [13] S.M. Muyeen, M.A. Mannan, M.H. Ali, R. Takahashi, T. Murata, J. Tamura, "Stabilization of Grid Connected Wind Generator by STATCOM", IEEE Power Electronics and Drives Systems, vol. 2, 2005
- [14] L. Chun, J. Qirong, X. Jianxin, "Investigation of Voltage Regulation Stability of Static Synchronous Compensator in Power System", IEEE Power Engineering Society Winter Meeting, vol. 4, pp.2642-2647, 2000
- [15] Kunder P., " Power System Stability and Control", the EPRI Power System Engineering Series, McGraw-Hill, New Yourk,1994.
- [16] N. Mohan, T. Undeland, and W. Robbins., " Power Electronics Converters, Applications, and Design", New York, Wiley, 2003.
- [17] P. Dusan, "Use of HVDC and FACTS", Proc. of the IEEE, vol. 88, no. 2, pp. 235–245, 2000.
- [18] Lie Xu Liangzhong Yao Sasse, C., "Comparison of Using SVC and STATCOM for Wind Farm Integration", International Conference on Power System Technology, Power Con., pp. 1-7, 2006.
- [19] S. M. Bamasak and M. A Abido, "Assessment Study Of Shunt Facts-Based Controllers Effectiveness On Power System Stability Enhancement", 39th UPEC Proceedings, vol. 1, pp 65-71, 2004.
- [20] A.H.M.A. Rahim, S.A.Al-Baiyat, and F.M. Kandlawala. "A robust STATCOM controller for power system dynamic performance enhancement", IEEE power engineering Society Summer Meeting, Vancouver, Canada, 2001.

- [21] A.H.M.A. Rahim and F.M. Kandlawala. ,“A robust design of a power system STATCOM controller using loop-shaping Technique”, Saudi engineering society conference, 2002.
- [22] Stella Morris, P.K. Dash, K.P. Basu, “A fuzzy variable structure controller for STATCOM.”, Int, Electric Power System Research, 2003.
- [23] N. Mithulananthan, C. Canizares, J. Rooeve, and G. Rogers, “Comparison of PSS, SVC, and STATCOM for Damping Power System Oscillations”, IEEE Trans. On Power Systems, vol. 18, no. 2, 2003.
- [24] M. Z. El-Sadek, “Power System Control”, Muchtar press- Assiut- Egypt, 2004.
- [25] Claudio A. Canizares, "Power Flow and Transient Stability Models of FACTS Controllers for Voltage and Angle Stability Studies ", National Science and Engineering Research Council (NSERC), Canada, Jan., 2000.
- [26] C. A. Canizares and Z. T. Faur, "Analysis of SVC and TCSC Controllers in Voltage Collapse," IEEE Trans. Power Systems, Vol. 14, No. 1, pp. 158-165, Feb., 1999.
- [27] E. Larsen, S. Nilsson, N. Miller, and S. Lindgren, “Benefits of GTO-based compensation systems for electric utility applications,” IEEE Trans. Power Delivery, Vol. 7, No. 4, pp. 2056–2062, Oct., 1992.
- [28] E. Uzunovic, C. A. Canizares, J. Reeve, "Fundamental Frequency Model of Static Synchronous Compensator", in: Proc. North American Power Symposium (NAPS), Laramie, Wyoming, pp. 49–54, 1997.
- [29] C. Schauder, M. Gernhardt, E. Stacey, T. Lemak, L. Gyugyi, T. W. Cease, A. Edris, "Development of a ± 100 MVar Static Condenser for Voltage Control of Transmission Systems", IEEE Trans. Power Delivery Vol. 10, No. 3, pp. 1486–1493, 1995.
- [30] P. K. Steimer, H. E. Gruning, J. Werninger, E. Carrol, S. Klaka, S. Linder, "IGCT-A New Engineering Technology for High Power, Low Cost Inverters", IEEE Industry Applications Magazine, pp.12–18, 1999.
- [31] D. N. Koseterev, "Modeling Synchronous Voltage Source Converters in Transmission System Planning Studies", IEEE Trans. Power Delivery Vol.12, No.2, pp. 947–952, 1997.
- [32] C. A. Canizares, E. Uzunovic, J. Reeve, and B. K. Johnson, "Transient Stability Models of Shunt and Series Static Synchronous Compensators," IEEE Trans., Power Delivery, Dec., 1998.

APPENDICES

Wind Turbine Induction Generator WTIG Parameters

Turbine: 3MW, base wind speed =9m/s, β controller $K_p=5$, $K_i=25$, $\beta_{max}=45^\circ$

Generator: $P=3.33$ MVA, $V=575$ V, $f=60$ Hz, $R_s=0.004843$, $L_s=0.1248$, $R_r=0.004377$,
 $L_r=0.1791$, $L_m=6.7$, $H=5.04$ s, $F=0.01$, $p=3$.

Transformer parameters: 47MVA, 120/25kV, $R_2=0.0026$, $L_2=0.08$, $R_m=500\Omega$, $X_m=500\Omega$.

WTIG to distribution network: 4MVA, 25kV/575V, $R_2=0.0008$, $L_2=0.025$, $R_m=500\Omega$, $X_m=inf$.

Transmission line parameters per km: $R_l=0.1153\Omega$, $R_0=0.413\Omega$, $L_l=1.05$ mH, $L_0=3.32$ mH, $C_l=11.33$ nF, $C_0=5.01$ nF.

STATCOM parameters: $25kV$, $3MVA$, $R=0.071$, $L=0.22$, $V_{dc}=4kV$, $C_{dc}=0.0011F$,
Regulator gains: $V_{ac}-K_p=5$, $K_i=1000$, $V_{dc}-K_p=0.0001$, $K_i=0.02$, $K_p=0.3$, $K_i=10$,
 $K_f=0.22$, $Droop=0.03$.

SVC parameters: $V_{rms}=25kV$, $F_n=60Hz$, $P_{base}=3MVA$, $Q_c=3Mvar$, $Q_l=-3Mvar$,
 $T_d=4msec$, $V_{ref}=1.0pu$, $X_s=0.03pu$, $K_p=0$, $K_i=300$.

Inductive load: *First load:* $3MW+J1Mvar$, *Second load:* $5MW+J2Mvar$

Plant: $2MVA$, $V=2.3kV$, $R_L=200KW$, $P.F=0.93$ Lag., $Q_c=800Kvar$

Induction Motor: $P=1.86MVA$, $V=2300V$, $f=60Hz$, $R_s=0.0092$, $L_s=0.0717$,
 $R_r=0.007$, $L_r=0.0717$, $L_m=4.14$, $H=0.5s$, $F=0$, $p=2$.

تأثيرات نظم نقل التيار المتردد المرنة على المولدات الحثية المداره بتوربينات الرياح

يتناول البحث موضوعاً مهماً في نظم القوى الكهربائية وهو دراسة تحسين أداء المولدات الحثية المداره بالرياح ويقدم البحث طرق مختلفة لتحسين أداء المولدات الحثية المداره بالرياح وأحداث إستقرار سريع للذبذبات التي تحدث في منظومة القوى الكهربائية نتيجة الإضطرابات الفجائية التي تتعرض لها منظومة القوى الكهربائية. كما تناول البحث عرض نموذج رياضى كامل لمكونات عناصر منظومة القوى الكهربائية والبحث يقترح دراسة دمج كلا من معوضات القدره الغير الفعاله الأستاتيكيه ومكثفات التزامن الأستاتيكيه على المولدات الحثية المداره بالرياح عند وجود الأضطرابات الفجائيه مثل حدوث تغيير في سرعة الرياح، حدوث قصر بين وجهين والأرض على إحدى أطراف المولدات الحثيه، حدوث قصر بين ثلاثة أوجه والأرض على قضبان التوزيع، حدوث تغيير مفاجئ في حمل حثى بالزيادة وبالنقصان وأخيرا توصيل محطة تحنوى على محرك حثى ثلاثى الأوجه ومكثف متصل على التوازي مع المحرك لتحسين معامل قدرته وكذلك حمل مادي.